

## CFTR Activation By Roflumilast Contributes to Therapeutic Benefit in Chronic Bronchitis

James A Lambert<sup>1,6</sup>, S Vamsee Raju<sup>1</sup>, Li P Tang<sup>1,5</sup>, Carmel M McNicholas<sup>3</sup>,  
Yao Li<sup>1,5</sup>, Clifford W Courville<sup>1</sup>, Roopan F Faris<sup>1,2</sup>, George E Coricor<sup>6</sup>, Lisa H  
Smoot<sup>1</sup>, Marina M Mazur<sup>5</sup>, Mark T Dransfield<sup>1,4</sup>, Graeme B Bolger<sup>1,7</sup>, Steven M  
Rowe<sup>1,2,3,4,5</sup>

Departments of Medicine<sup>1</sup>, Pediatrics<sup>2</sup>, Cell, Integrative, and Developmental  
Biology<sup>3</sup>, Pharmacology<sup>7</sup>, the UAB Lung Health Center<sup>4</sup>, the Cystic Fibrosis  
Research Center<sup>5</sup>, and the Department of Biochemistry and Structural Biology<sup>6</sup> at  
University of Alabama at Birmingham, Birmingham, Alabama, USA

Corresponding Author:

Steven M Rowe, MD MSPH

MCLM 768 1918 University Blvd

Birmingham, AL 35294-0006

Phone: (205) 934-9640

Fax: (205) 934-7593

smrowe@uab.edu

"This article has an online data supplement, which is accessible from this issue's  
table of content online at [www.atsjournals.org](http://www.atsjournals.org)"

**Grant Funding:** This research was sponsored by the NIH: 1R01 HL105487 to S.M.R., and P30 DK072482 to the UAB CF Research Center, the CFF (R464) and Forest Research Institute. J.A.L. was supported by the Howard Hughes Medical Institute. S.V.R. was supported by the American Lung Association Senior Research Fellowship (RT-219427-N).

**Running Title:** CFTR Activation by Roflumilast in Chronic Bronchitis

**Word Count:** 3655

**Abstract Count:** 242

**Method Count:** 500

*At a Glance Commentary*

**Scientific Knowledge on the Subject:** Cigarette smoke decreases CFTR activity in the airway of COPD patients, leading to mucus stasis and chronic bronchitis. Roflumilast is a clinically approved cAMP-selective phosphodiesterase inhibitor that improves outcomes in COPD patients with chronic bronchitis and frequent respiratory exacerbations, and could activate CFTR by elevating cAMP.

**What This Study Adds to the Field:** Roflumilast activates CFTR by elevating cAMP levels, and mitigates acquired CFTR dysfunction caused by cigarette smoke, providing a potential mechanism by which it confers therapeutic benefit among COPD patients with chronic bronchitis. Roflumilast also activates CFTR

in intestinal epithelia, which may contribute to non-infectious diarrhea, a known side effect of the drug.

This article has an online data supplement, which is accessible from this issue's table of content online at [www.atsjournals.org](http://www.atsjournals.org)

**Abstract**

**RATIONALE:** Cigarette smoking causes acquired CFTR dysfunction and is associated with delayed mucociliary clearance and chronic bronchitis.

Roflumilast is a clinically approved phosphodiesterase4 inhibitor that improves lung function in patients with chronic bronchitis. We hypothesized its therapeutic benefit was related in part to activation of CFTR.

**METHODS:** Primary human bronchial epithelial (HBE) cells, Calu-3, and T84 monolayers were exposed to whole cigarette smoke (WCS) or air, with or without roflumilast. CFTR-dependent ion transport was measured in modified Ussing chambers. ASL was determined by confocal microscopy. Intestinal fluid secretion of ligated murine intestine was monitored *ex vivo*.

**RESULTS:** Roflumilast activated CFTR-dependent anion transport in normal HBE cells with an  $EC_{50}$  of 2.9 nM. Roflumilast partially restored CFTR activity in WCS-exposed HBE cells ( $5.3 \pm 1.1 \mu A/cm^2$  vs. control  $1.2 \pm 0.2$ ,  $P < 0.05$ ) and was additive with ivacaftor, a specific CFTR potentiator approved for CF. Roflumilast improved depleted ASL depth of HBE monolayers exposed to WCS ( $9.0 \pm 3.1 \mu m$  vs.  $5.6 \pm 2.0$  control,  $P < 0.05$ ), achieving 79% of that observed in air controls. CFTR activation by roflumilast also induced CFTR-dependent fluid secretion in murine intestine, increasing wet/dry ratio and diameter of ligated murine segments.

CONCLUSIONS: Roflumilast activates CFTR-mediated anion transport in airway and intestinal epithelia via a cAMP-dependent pathway and partially reverses the deleterious effects of WCS, resulting in augmented ASL depth. Roflumilast may benefit COPD patients with chronic bronchitis by activating CFTR, which may also underlie non-infectious diarrhea caused by roflumilast.

**Author Contributions:**

J.A.L., S.V.R., M.T.D., G.B.B., and S.M.R. conceived of the experiments; J.A.L., S.V.R., C.M. M., L.P.T., Y.L., C.W.C., R.F.F., G.E.C., L.H.S., and M.M.M. conducted research; J.A.L., S.V.R., Y.L., C.W.C., G.B.B., and S.M.R. analyzed the data; J.A.L., S.V.R., and S.M.R. wrote the manuscript; S.M.R. supervised the project.

## Introduction

Chronic obstructive pulmonary disease (COPD) is the third leading cause of death in the US and shares many pathologic features with CF airway disease (1, 2). This is particularly true for individuals that exhibit chronic bronchitis, which occurs in the majority of individuals with COPD (3). Cystic fibrosis (CF) is caused by defects in the cystic fibrosis transmembrane conductance regulator (CFTR), a cAMP-regulated anion transporter expressed on the apical surface of epithelial cells in multiple tissues, including the lung and intestine (4). Due to the absence of functional CFTR in CF patients, airway surface liquid (ASL) depletion results (5), contributing to delayed mucociliary clearance (MCC), bacterial colonization, and respiratory decline (4). Patients with COPD also exhibit delayed MCC and mucus retention which are independently associated with increased mortality (6) and accelerated disease progression (7).

Recently, a number of laboratories have shown that acquired CFTR dysfunction may cause delayed MCC, even in the absence of congenital CFTR mutations (2, 8, 9). Cigarette smoke has been shown to reduce CFTR expression (9), increase CFTR internalization (10), and disrupt CFTR ion channel function in airway epithelial monolayers (9). Cigarette smoke also acutely decreases CFTR activity in the nasal airway, inducing rapid cellular internalization (10). The net effect is severely reduced CFTR-mediated fluid transport, depletion of the ASL and delayed MCC (2). Clinical studies using nasal potential difference (NPD) show that cigarette smoking is associated with reduced CFTR activity in healthy

smokers and COPD smokers, even in the absence of CFTR mutations(2, 8), a finding recapitulated in the lower airway(11). Reduced CFTR function in the nose and lung were also associated with chronic bronchitis(2, 11), suggesting CFTR could represent a potential therapeutic target.

Cyclic nucleotidephosphodiesterase(PDE) inhibitors increase cellular cAMPand/or cGMP(12).The cAMP-selective PDE4 family is a majorisoform found in respiratory epitheliaand resident immune cellsof the lung(13, 14).Roflumilast is a PDE4-selective inhibitorthatimproves lung function andthe number of pulmonary exacerbations in patients with COPD, although only in patients with chronic bronchitisand frequent exacerbations(15).Whyroflumilast improves this specific patient sub-phenotyperemains largely unknown, and its effect on ion transport has not been characterized.Given that PDE inhibitors are known to strongly increase the chloride transport activity of CFTR(16), which would be expected to augment MCC, we hypothesized thatroflumilast may ameliorate acquiredCFTR dysfunctionby inducing PKA-mediated CFTR phosphorylation of residual CFTR, augmenting epithelial function in individuals with chronic bronchitis.CFTR-dependent fluid secretion could also be the basis of non-infectious diarrhea commonly associated with roflumilast treatment (17). Using epithelial monolayers and murine tissues, we determined the effects of roflumilast following whole cigarette smoke (WCS) exposure. Our studies demonstrate roflumilast activates CFTR-dependent chloride secretion and abrogatesthe deleterious effects caused by WCS, while also contributing to gastrointestinal fluid secretion in a CFTR-dependent fashion. These results

suggest roflumilast confers clinical benefit in COPD patients by activating CFTR, and reiterate the importance of this pathway in COPD therapeutics.

## **Methods**

### *Procurement and Growth of Epithelial Cells*

Use of primary human bronchial epithelial cells (HBE) and tissues were approved by the Institutional Review Board. HBE cells were obtained from lung explants and garnered from normal donors and confirmed to lack CFTR mutations (2, 18, 19). First or second passage cells were grown until terminally differentiated (2, 18, 19). Calu-3 and T84 monolayers were grown at air liquid interface(16).

### *Whole Cigarette Smoke Exposure*

Cells were subjected to 3R4F (University of Kentucky) WCS exposure levels via an inExpose cigarette pump system (Scireq-USA, Tempe, AZ) at 3L/minute using flexiWare6 software. Machined containers were used to expose monolayers to WCSfor 10- 30 minutes. Air control monolayers were placed in a cleanair current chamber replica.

### *Voltage Clamp Studies in Ussing Chambers*

Short-circuit current (I<sub>sc</sub>) was measured under voltage clamp conditions using MC8 voltage clamps and P2300 Ussing chambers (Physiologic Instruments, San

Diego, CA) as previously described (2, 19). Chambers were maintained at 37°C and 5% CO<sub>2</sub>. Mucosa of intact bronchus were performed similarly(2).

#### *cAMP Quantitation and CFTR Regulatory Region Phosphorylation*

cAMP was measured in Calu-3 cells with an EIA kit (Cayman Chemical Company Ann Arbor, MI). R-region phosphorylation was performed in COS7 cells as described(20). COS7 cells were transfected transiently with a plasmid encoding the CF R-region (amino acids 635-836) with an N-terminal HA epitope tag. Following 24 hr treatment, lysates were immunoblotted with an anti-HA monoclonal antibody (R+D systems, Minneapolis, MN) to detect R-region phosphorylation.

#### *Airway Surface Liquid (ASL) Depth*

The apical surface of HBE cells were stained with Texas red dye (20 µl at 2 mg/ml in Fc70) and cells labeled with CMFDA (100 µM) approximately 4 hrs prior to imaging. ASL depth was imaged with a confocal microscope and XZ scans. Values for each monolayer were derived from 4 regions of interest(2).

#### *Intestinal Secretion Assay*

Adult AJ mice were euthanized and the small intestine removed and bathed in MEM. Intestine was flushed with saline solution to remove fecal deposits, then sequential 10 cm segments were ligated. Intestinal segments were

then placed in media with either roflumilast (30 nM), forskolin (20  $\mu$ M), or vehicle at 37°C and 95% O<sub>2</sub>/5% CO<sub>2</sub> for 3 hours. Weight and diameter measurements were taken prior to addition of compounds and hourly thereafter. Upon completion, segments were desiccated to calculate wet/dry ratio and data normalized by experimental day. Diameters were calculated by image analysis by an investigator blinded to treatment assignment.

#### *Western blot analysis of CFTR expression.*

CFTR expression in primary HBE cells treated with DMSO vehicle control or 30 nM of roflumilast was carried out according to the previously published protocols (2, 21).

#### *Unitary conductance tracings.*

Single channel currents were recorded from inside-out patches of primary HBE cells expressing wild-type CFTR treated with PKA + ATP alone or PKA + ATP + roflumilast and open probability was calculated as reported previously (21, 22).

#### *Reagents*

Roflumilast (FW 403.21) was obtained from Santa Cruz (Dallas, Texas, USA, Cat. #208313) and dissolved in DMSO at 1000 fold stock concentration. H89 was from Enzo (Farmingdale, NY). All other agents were obtained from Sigma-Aldrich (St. Louis, MO). CSE was prepared as described (2).

### Statistics

Inferential comparisons made using Student's t-test or ANOVA, as appropriate. Post-hoc tests for multiple comparisons were calculated using Fisher's least significant difference. All statistical tests were two-sided and were performed at a 5% significance level using GraphPad Prism (La Jolla, CA). Error bars designate SEM unless indicated otherwise.

### Results

#### **Cigarette Smoke decreases CFTR-dependent ion transport in HBE cells.**

*In vitro* WCS exposure represented physiologically relevant concentrations of particulate matter that was comparable to that observed in smokers(23), as described in online supplement. To characterize dose-dependent effects of WCS induced lung injury, we tested various levels of exposure on forskolin-stimulated transepithelial chloride transport in non-CF HBE monolayers. WCS caused a significant and dose-dependent reduction in CFTR-dependent ion transport (Fig. 1A,B) that was similar in magnitude to prior studies using cigarette smoke extract(CSE)(2). Transepithelial resistance (TER) of HBE monolayers was not affected following 10 and 20 min exposure durations, although TER was reduced by WCS exposure following the highest (30 min) exposure intensity (Fig. 1C).

Since the CFTR-dependent ion transport decrement observed at 10 and 20 min WCS exposures resembled that seen *in vivo* (2, 8, 24), these exposures were used for subsequent studies while also avoiding non-specific epithelial injury (e.g. decreased TER) seen with longer durations.

### **Roflumilast activates CFTR-dependent anion transport by increasing cAMP and R-Region phosphorylation.**

To quantify the effects of roflumilast on CFTR function, we established the dose dependence of roflumilast on anion transport in primary HBE monolayers (Fig. 2A,B). Roflumilast activated cAMP-dependent CFTR anion transport in primary non-CF HBE monolayers with an  $EC_{50}$  of 2.9 nM, reaching a maximal current of  $38.9 \pm 6.2 \mu A/cm^2$  at 30 nM. Based on these results, we used 30 nM roflumilast, a concentration expected to occur in humans (25) while also conferring activity of at least 90% of the  $EC_{max}$ . Roflumilast also activated CFTR-dependent currents in freshly excised human bronchi derived from a healthy donor ( $EC_{50} = 10.6$  nM, Fig. 2C,D) in a fashion similar to epithelial monolayers. Roflumilast (30 nM) had no effect on CF HBE cells derived from a F508del homozygote with no detectable surface CFTR expression ( $2.5 \pm 0.7 \mu A/cm^2$  roflumilast vs  $4.3 \pm 0.9 \mu A/cm^2$  vehicle). Roflumilast activated CFTR in a mechanism that was similar to forskolin, an adenylate cyclase activator that also increases cellular cAMP levels. Roflumilast did not produce any additional  $I_{sc}$  stimulation over that conferred by maximal forskolin addition (20  $\mu M$ ), and the two compounds did not exhibit additive effects on CFTR-dependent anion transport in

Calu-3 monolayers (Fig. 2E,F). As expected, roflumilast increased intracellular cAMP ( $0.30 \pm 0.16$  pmol/ml roflumilast, vs.  $0.10 \pm 0.02$  pmol/ml control,  $P < 0.05$ ; Fig. 3A), consistent with its function as a PDE4 inhibitor.

To further identify the mechanism of action, we tested the effects of roflumilast on the phosphorylation of isolated CFTR Regulatory Region (R-R). We have shown previously that this assay is a sensitive measure of the phosphorylation of the CFTR R-R by the cAMP-dependent protein kinase A (PKA) (20). Roflumilast induced robust phosphorylation of isolated CFTR R-R in a dose-dependent fashion that was sensitive to the PKA inhibitor H89 (Fig. 3B). The  $EC_{50}$  for phosphorylation in this assay was at a concentration similar to the  $IC_{50}$  of enzyme inhibition, indicating that the pharmacologic action of roflumilast was consistent with enzyme inhibition.

Since, increased  $I_{sc}$  could also be product of increased surface expression or direct effect on CFTR open channel probability ( $P_o$ ), we tested whether roflumilast altered the expression of CFTR or had any direct effects on the channel function by Western blot analysis and unitary conductance tracings, respectively. In HBE cells treated with roflumilast for 24 hours, CFTR expression remained comparable to what was found in cells treated with vehicle control (Supplementary Fig. 2). In addition, single channel studies with isolated membrane patches from HBE cells indicate that roflumilast does not alter the  $P_o$  of CFTR (Supplementary Fig. 3). In combination, these results indicate that roflumilast activates CFTR by elevating cAMP, inducing phosphorylation of R-R

through a PKA-dependent pathway, without significantly altering surface expression.

### **Roflumilast ameliorates smoke-induced CFTR dysfunction**

To evaluate whether roflumilast could ameliorate the deleterious effects of WCS on CFTR activity, we subjected HBE monolayers to WCS and evaluated the effect of roflumilast in Ussing chambers. Roflumilast significantly increased  $I_{sc}$  compared to vehicle control in monolayers exposed to WCS for 10 min ( $5.3 \pm 1.1 \mu A/cm^2$  roflumilast vs.  $1.2 \pm 0.2 \mu A/cm^2$  control,  $P < 0.05$ ); when expressed as a fraction of maximal CFTR stimulus induced by forskolin, roflumilast activated  $I_{sc}$  to 47.3% and 30.2% in air and WCS exposed monolayers, respectively (Fig. 4A). Similar beneficial effects were observed following 20 min WCS exposures (Fig. 4B). Roflumilast caused a  $6.6 \pm 2.2 \mu A/cm^2$  stimulation in anion transport in WCS exposed cells compared to  $0.5 \pm 1.2 \mu A/cm^2$  in vehicle treated cells ( $P < 0.05$ ), which was equivalent to 33.9% of the maximal forskolin response in smoke exposed cells. The CFTR potentiator ivacaftor (formerly VX-770) has also been reported to ameliorate the deleterious effects of WCS exposure on anion transport (2). As opposed to roflumilast, activation of CFTR by ivacaftor is cAMP independent (26), providing an alternative mechanism by which acquired CFTR dysfunction could be addressed. To test for additive benefit, we evaluated these agents alone and in combination. In WCS exposed HBE cells, roflumilast and ivacaftor augmented CFTR-dependent ion transport to similar levels, but had an

additive effect when combined (Fig. 4C). Taken together, these studies demonstrated that roflumilast significantly mitigated WCS-induced CFTR dysfunction in a cAMP-dependent fashion, warranting further evaluations to detect downstream effects of roflumilast on epithelial function.

### **Roflumilast increases airway surface liquid depth in WCS-exposed cells.**

Since CFTR secretes chloride ions to regulate ASL depth, an important determinant of normal MCT (27), we next evaluated whether roflumilast augmented ASL depth in WCS exposed monolayers using confocal microscopy. Consistent with previous observations (2, 10), WCS decreased ASL depth compared to control monolayers ( $5.6 \pm 2.0 \mu\text{m}$  WCS vs.  $11.4 \pm 4.1 \mu\text{m}$  air control,  $P < 0.05$ ). Roflumilast treatment significantly mitigated WCS induced reductions in ASL depth ( $9.0 \pm 3.1 \mu\text{m}$  roflumilast vs  $5.6 \pm 2.0 \mu\text{m}$  vehicle,  $P < 0.05$ ), reaching 79% of the ASL depth found in normal HBE monolayers (Fig. 5).

### **Roflumilast increases CFTR activity of intestinal monolayers *in vitro* and intestinal segments *ex vivo*.**

Roflumilast therapy is associated with non-infectious diarrhea, and the cause for this adverse reaction has not yet been determined. Because CFTR is highly expressed in gut epithelia and its activation can contribute to diarrhea, we hypothesized roflumilast might cause diarrhea by augmenting CFTR-dependent fluid secretion. Roflumilast significantly increased CFTR-dependent anion

transport of T84 intestinal epithelial monolayers compared to vehicle ( $1.5 \pm 0.4 \mu\text{A}/\text{cm}^2$  roflumilast vs.  $-1.0 \pm 0.7 \mu\text{A}/\text{cm}^2$  vehicle;  $P < 0.05$ , Fig. 6A,B). In isolated murine intestinal segments, roflumilast increased fluid secretion as reflected by increased wet/dry ratio ( $6.4 \pm 0.8$  roflumilast vs.  $5.6 \pm 0.7$  vehicle,  $P < 0.005$ ; Fig. 6C,D) and change in intestinal diameter ( $0.10 \pm 0.01$  mm roflumilast vs.  $0.06 \pm 0.01$  mm vehicle,  $P < 0.05$ ; Fig 6E). No effect of roflumilast was observed in ligated intestine derived from CFTR (-/-) mice (Congenic  $\text{Cftr}^{\text{tm1Unc/J}}$ ) (Fig. 6D,E). These data illustrate that CFTR activation in intestinal epithelia by roflumilast could underlie the non-infectious diarrhea observed during roflumilast therapy.

## Discussion

Emerging data from several laboratories indicate that cigarette smoke causes CFTR dysfunction *in vitro* and *in vivo* even in the absence of inherited CFTR mutations. This has been suggested to contribute to COPD pathogenesis by causing a predisposition to epithelial dysfunction (2, 9, 21, 24), mucus retention (2, 21, 28), and chronic bronchitis (2, 11, 21), resulting in a phenotype that resembles mild CF. Our studies are consistent with this hypothesis, and demonstrate a 30-40% reduction in CFTR activity following WCS exposure without significant deleterious effect on transepithelial resistance or other indicators of cellular toxicity. This is similar to published studies using cigarette

smoke extract (CSE) (2, 8, 9) and WCS (24, 29), and also resembles the magnitude of CFTR decrement detected in the upper (2, 8) and lower airway (11) of cigarette smokers. CFTR inhibition by WCS was dose-dependent, providing additional confidence in the causative nature of cigarette smoke exposure. Furthermore, particulate analysis of the 10 and 20 min WCS exposures demonstrate a clinically relevant. The degree of CFTR inhibition by WCS was sufficient to reduce ASL depth, which is known to decrease the efficiency of MCT (30). Since the severity of the ion transport and ASL abnormalities were intermediate compared to the defect observed in CF epithelial cells, it seems likely this decrement is sufficient to initiate a cascade of mucus retention and infection *in vivo*, particularly if present over multiple years and combined with enhanced mucus expression also caused by cigarette smoking (2, 31).

Recent studies have shown agents that activate CFTR, such as the CFTR potentiator ivacaftor, augment ASL depth and consequently accelerate MCC, pharmacologically reversing acquired CFTR dysfunction (2). Alternatively, hypertonic saline, which compensates for CFTR-dependent ASL decrements, also restores ASL volume by osmotic forces (24) and reduces mucus obstruction in a mouse model of chronic bronchitis (32). Since PDE4 inhibitors are known to increase intracellular levels of cAMP and activate CFTR in airway epithelia (33-38), we hypothesized roflumilast could act similarly and ameliorate acquired CFTR dysfunction conferred by cigarette smoke exposure. As shown in our studies, roflumilast efficiently activated CFTR in both primary HBE cells and

intact human tissues, two models highly faithful to the ion transport properties of human airway epithelia *in vivo*(2, 26). In both cells and tissues, the  $EC_{max}$  of roflumilast-mediated CFTR activation was ~30 nM, and exhibited a broad therapeutic plateau without signs of cellular toxicity or rundown. These concentrations are therapeutically relevant, and are routinely achieved in humans prescribed roflumilast for therapeutic purposes, suggesting wild-type CFTR activation could be readily achieved by therapeutic doses of roflumilast *in vivo*(25). The effects of roflumilast on CFTR function were also observed in epithelial cells exposed to WCS, indicating acquired CFTR dysfunction is a relevant therapeutic target that can be addressed with roflumilast. Roflumilast robustly activated CFTR following both low and moderate cigarette smoke exposures. Consequently, reduced ASL depth conferred by WCS exposure was significantly ameliorated by co-treatment with roflumilast. By enhancing ASL depth by CFTR-mediated fluid secretion, improved MCT is anticipated(2, 30), which could enable a more robust host defense in the COPD airway.

Roflumilast reduces the frequency of COPD exacerbations in patients who exhibit chronic bronchitis and have a history of frequent exacerbations(39). However, the mechanisms of its therapeutic properties are not yet completely understood. Roflumilast and other PDE4 inhibitors exhibit anti-inflammatory properties, including the reduction of matrix metalloproteinase (MMP) activity and TGF-beta-1 release following lung injury(17, 40). While these mechanisms may confer benefit in patients with COPD, it is not clear why patients who have emphysema, and consequently significant inflammation even

in the absence of chronic mucus hypersecretion, are not affected by this cAMP-mediated mechanism of inflammation. Conversely, two previous studies in distinct patient cohorts demonstrated CFTR dysfunction among COPD patients was associated with chronic bronchitis(2, 11). Since roflumilast activates residual CFTR function, and there is a strong association between CFTR abnormality and bronchitis(2, 11), it is likely that CFTR activation may be partially responsible for the therapeutic efficacy of roflumilast. Further studies are warranted to confirm this hypothesis, and may also benefit from animal models of chronic bronchitis to address these questions.

Our data indicate a mechanistic basis underlying non-infectious diarrhea associated with roflumilast therapy. As a cAMP activated Cl<sup>-</sup> channel expressed prominently in the intestine, CFTR has long been postulated to have an active role in secretory diarrhea(41). Although CFTR probably does not contribute to nausea caused by roflumilast, which is likely related to inhibition of PDE4D in neurons that regulate nausea(42), our studies demonstrate that roflumilast strongly activates CFTR in the distal intestine, leading to fluid secretion into the lumen. Studies in CFTR knockout mice confirmed this was CFTR-dependent, and establish that CFTR contributes to intestinal secretion when activated. Since CFTR inhibitors are presently being developed for the treatment of diarrhea(19, 43), it may be possible to abrogate the undesirable effects of roflumilast on the lower GI tract by co-administering oral CFTR inhibitors that are not systemically absorbed. This strategy is worthy of further exploration as a therapeutic

approach to minimize the adverse effects of roflumilast while also allowing maximal benefit in the lung to be achieved.

Roflumilast activated CFTR by increasing levels of cAMP, resulting in a PKA-dependent phosphorylation of CFTR, a crucial step towards activating CFTR-mediated anion transport(20, 25, 34). As such, roflumilast activates CFTR in a fashion similar to forskolin, which explains why roflumilast did not potentiate maximal forskolin activity. "Further, its effects are dependent on some residual CFTR residing at the membrane despite smoking induced lung injury, since it does not alter the levels of CFTR at the membrane. Several studies demonstrate that sufficient CFTR (nearly 50-60%) is present at the cell surface in COPD patients, and thus could serve as a therapeutic target in this way (2, 10, 21, 44). In contrast to roflumilast, ivacaftor potentiates CFTR activation by uncoupling ATPase activity from channel gating(26, 45, 46) and exhibits the most efficient pharmacological potentiation of wild type CFTR in the setting of submaximal forskolin pre-activation(2). This explains why roflumilast-mediated CFTR activation was additive to ivacaftor, since the mechanism of these agents are distinct and complementary. Combination treatment could represent a potential approach to maximize CFTR activation among patients with deficient CFTR function, including those with acquired abnormalities of CFTR activity. Whether this could also be helpful in individuals with partially active CFTR alleles localized to the cell surface also deserves further exploration.

While the data provide evidence supporting CFTR activation as a basis for the beneficial effects of roflumilast, important limitations of the study should be

noted. Although WCS has been frequently used to model smoking-related lung disease(24, 29), and reduced CFTR function observed here is consistent with prior studies(2, 9, 24, 29), the experiments conducted rely on acute cigarette smoke exposure, and are unlikely to capture the complexity of the airway environment in COPD patients, such as airway inflammation, disrupted proteolytic balance, and ER stress (3, 31, 47, 48). While it seems reasonable to invoke that CFTR activation by roflumilast contributes to therapeutic benefit in patients with chronic bronchitis, and is supported by specificity controls, as an efficacious activator of intracellular cAMP, roflumilast may also improve the function of surface epithelia via other pathways. For example, cAMP is known to stimulate CFTR trafficking to the membrane(49), inhibit MUC5AC expression (50), and is also an important stimulus of ciliary beating(51), which could augment mucociliary clearance. Moreover, roflumilast also has strong anti-inflammatory effects including inhibition of both p38 MAP kinase (17, 52), oxygen radical production (53) as well as suppression of the proliferation and cytokine release from CD4<sup>+</sup>, CD8<sup>+</sup> lymphocytes that may be involved in the inhibition of the pro-inflammatory transcription factor NF- $\kappa$ B(52). Murine intestines are frequently used models for CFTR biology in the intestine, and provide an important specificity control regarding the effects of roflumilast; however, it is certainly plausible that other cAMP-mediated ion channels could contribute to secretory diarrhea induced by roflumilast in humans. Further studies, including the co-administration of specific CFTR inhibitors in more sophisticated animal models, may help rule out this possibility.

In summary, acquired CFTR dysfunction caused by WCS can be ameliorated by roflumilast-mediated activation of cAMP/PKA-dependent CFTR activation, resulting in improved epithelial function. CFTR activation may underlie the beneficial effects of roflumilast in COPD patients with chronic bronchitis, and also contribute to secretory diarrhea by hyperactivation of the same pathway. Additional studies to define the role of CFTR activation by roflumilast are needed in COPD, and could result in improved therapeutic strategies to address acquired CFTR dysfunction in smoking-related lung disease while blocking its undesirable adverse effects.

## **Acknowledgements**

The authors acknowledge the efforts of Ming Du and David Bedwell for supplying CF and non-CF mice through the UAB CF Center Animal Core. We are also grateful to Jeremy A Boyston and John E Trombley for assistance with WCS exposure analytics.

## References

1. Calverley PM, Walker P. Chronic obstructive pulmonary disease. *Lancet* 2003;362(9389):1053-1061.
2. Sloane PA, Shastry S, Wilhelm A, Courville C, Tang LP, Backer K, Levin E, Raju SV, Li Y, Mazur M, et al. A pharmacologic approach to acquired cystic fibrosis transmembrane conductance regulator dysfunction in smoking related lung disease. *PLoS One* 2012;7(6):e39809.
3. Yoshida T, Tuder RM. Pathobiology of cigarette smoke-induced chronic obstructive pulmonary disease. *Physiol Rev* 2007;87(3):1047-1082.
4. Rowe SM, Miller, S. & Sorscher. Cystic fibrosis. *N Engl J Med* 2005(352):1992-2001.
5. Matsui H, Grubb BR, Tarran R, Randell SH, Gatzky JT, Davis CW, Boucher RC. Evidence for periciliary liquid layer depletion, not abnormal ion composition, in the pathogenesis of cystic fibrosis airways disease. *Cell* 1998;95(7):1005-1015.
6. Hogg JC, Chu F, Utokaparch S, Woods R, Elliott WM, Buzatu L, Cherniack RM, Rogers RM, Sciurba FC, Coxson HO, et al. The nature of small-airway obstruction in chronic obstructive pulmonary disease. *N Engl J Med* 2004;350(26):2645-2653.
7. Vestbo J, Prescott E, Lange P. Association of chronic mucus hypersecretion with fev1 decline and chronic obstructive pulmonary disease morbidity. Copenhagen city heart study group. *Am J Respir Crit Care Med* 1996;153(5):1530-1535.
8. Cantin AM, Hanrahan JW, Bilodeau G, Ellis L, Dupuis A, Liao J, Zielenski J, Durie P. Cystic fibrosis transmembrane conductance regulator function is suppressed in cigarette smokers. *Am J Respir Crit Care Med* 2006;173(10):1139-1144.
9. Kreindler JL, Jackson AD, Kemp PA, Bridges RJ, Danahay H. Inhibition of chloride secretion in human bronchial epithelial cells by cigarette smoke extract. *Am J Physiol Lung Cell Mol Physiol* 2005;288(5):L894-902.
10. Clunes LA, Davies CM, Coakley RD, Aleksandrov AA, Henderson AG, Zeman KL, Worthington EN, Gentsch M, Kreda SM, Cholon D, et al. Cigarette smoke exposure induces cfr internalization and insolubility, leading to airway surface liquid dehydration. *FASEB J* 2011.
11. Dransfield MT, Wilhelm AM, Flanagan B, Courville C, Tidwell SL, Raju SV, Gaggar A, Steele C, Tang LP, Liu B, et al. Acquired cfr dysfunction in the lower airways in copd. *Chest* 2013.
12. Conti M, Beavo J. Biochemistry and physiology of cyclic nucleotide phosphodiesterases: Essential components in cyclic nucleotide signaling. *Annual review of biochemistry* 2007;76:481-511.
13. Dent G, White SR, Tenor H, Bodtke K, Schudt C, Leff AR, Magnussen H, Rabe KF. Cyclic nucleotide phosphodiesterase in human bronchial epithelial

- cells: Characterization of isoenzymes and functional effects of pde inhibitors. *Pulmonary pharmacology & therapeutics* 1998;11(1):47-56.
14. Barber R, Baillie GS, Bergmann R, Shepherd MC, Sepper R, Houslay MD, Heeke GV. Differential expression of pde4 camp phosphodiesterase isoforms in inflammatory cells of smokers with copd, smokers without copd, and nonsmokers. *American journal of physiology Lung cellular and molecular physiology* 2004;287(2):L332-343.
15. Calverley PM, Rabe KF, Goehring UM, Kristiansen S, Fabbri LM, Martinez FJ, M, groups Ms. Roflumilast in symptomatic chronic obstructive pulmonary disease: Two randomised clinical trials. *Lancet* 2009;374(9691):685-694.
16. Cobb BR, Fan L, Kovacs TE, Sorscher EJ, Clancy JP. Adenosine receptors and phosphodiesterase inhibitors stimulate cl- secretion in calu-3 cells. *American journal of respiratory cell and molecular biology* 2003;29(3 Pt 1):410-418.
17. Spina D. Pde4 inhibitors: Current status. *British journal of pharmacology* 2008;155(3):308-315.
18. Rowe SM, Miller S, Sorscher EJ. Cystic fibrosis. *The New England journal of medicine* 2005;352(19):1992-2001.
19. Sonawane ND, Hu J, Muanprasat C, Verkman AS. Luminally active, nonabsorbable cftr inhibitors as potential therapy to reduce intestinal fluid loss in cholera. *FASEB journal : official publication of the Federation of American Societies for Experimental Biology* 2006;20(1):130-132.
20. Pyle LC, Ehrhardt A, Mitchell LH, Fan L, Ren A, Naren AP, Li Y, Clancy JP, Bolger GB, Sorscher EJ, et al. Regulatory domain phosphorylation to distinguish the mechanistic basis underlying acute cftr modulators. *American journal of physiology Lung cellular and molecular physiology* 2011;301(4):L587-597.
21. Raju SV, Jackson PL, Courville C, Sloane PA, Tang LP, Dransfield MT, Rowe SM. Cigarette smoke induces systemic defects in cystic fibrosis transmembrane conductance regulator (cftr) function. *American journal of Respiratory Critical Care Medicine* 2013;Acceted for Publication.
22. Hickman-Davis JM, McNicholas-Bevensee C, Davis IC, Ma HP, Davis GC, Bosworth CA, Matalon S. Reactive species mediate inhibition of alveolar type ii sodium transport during mycoplasma infection. *American journal of respiratory and critical care medicine* 2006;173(3):334-344.
23. Schramm S, Carre V, Scheffler JL, Aubriet F. Analysis of mainstream and sidestream cigarette smoke particulate matter by laser desorption mass spectrometry. *Anal Chem* 2011;83(1):133-142.
24. Clunes LA, Davies CM, Coakley RD, Aleksandrov AA, Henderson AG, Zeman KL, Worthington EN, Gentsch M, Kreda SM, Cholon D, et al. Cigarette smoke exposure induces cftr internalization and insolubility, leading to airway surface liquid dehydration. *FASEB journal : official publication of the Federation of American Societies for Experimental Biology* 2012;26(2):533-545.
25. Rabe KF. Update on roflumilast, a phosphodiesterase 4 inhibitor for the treatment of chronic obstructive pulmonary disease. *British journal of pharmacology* 2011;163(1):53-67.

26. Van Goor F, Hadida S, Grootenhuis PD, Burton B, Cao D, Neuberger T, Turnbull A, Singh A, Joubran J, Hazlewood A, et al. Rescue of cf airway epithelial cell function in vitro by a cftr potentiator, vx-770. *Proceedings of the National Academy of Sciences of the United States of America* 2009;106(44):18825-18830.
27. Zhang L, Button B, Gabriel SE, Burkett S, Yan Y, Skiadopoulos MH, Dang YL, Vogel LN, McKay T, Mengos A, et al. Cftr delivery to 25% of surface epithelial cells restores normal rates of mucus transport to human cystic fibrosis airway epithelium. *PLoS biology* 2009;7(7):e1000155.
28. Innes AL, Woodruff PG, Ferrando RE, Donnelly S, Dolganov GM, Lazarus SC, Fahy JV. Epithelial mucin stores are increased in the large airways of smokers with airflow obstruction. *Chest* 2006;130(4):1102-1108.
29. Savitski AN, Mesaros C, Blair IA, Cohen NA, Kreindler JL. Secondhand smoke inhibits both cl- and k+ conductances in normal human bronchial epithelial cells. *Respir Res* 2009;10:120.
30. Matsui H, Randell SH, Peretti SW, Davis CW, Boucher RC. Coordinated clearance of periciliary liquid and mucus from airway surfaces. *Journal of Clinical Investigation* 1998;102(6):1125-1131.
31. Di YP, Zhao J, Harper R. Cigarette smoke induces muc5ac protein expression through the activation of sp1. *The Journal of biological chemistry* 2012;287(33):27948-27958.
32. Graeber SY, Zhou-Suckow Z, Schatterny J, Hirtz S, Boucher RC, Mall MA. Hypertonic saline is effective in the prevention and treatment of mucus obstruction but not airway inflammation in mice with chronic obstructive lung disease. *Am J Respir Cell Mol Biol* 2013.
33. Milara J, Armengot M, Banuls P, Tenor H, Beume R, Artigues E, Cortijo J. Roflumilast n-oxide, a pde4 inhibitor, improves cilia motility and ciliated human bronchial epithelial cells compromised by cigarette smoke in vitro. *British journal of pharmacology* 2012;166(8):2243-2262.
34. Moran O. Model of the camp activation of chloride transport by cftr channel and the mechanism of potentiators. *Journal of theoretical biology* 2010;262(1):73-79.
35. Barnes AP, Livera G, Huang P, Sun C, O'Neal WK, Conti M, Stutts MJ, Milgram SL. Phosphodiesterase 4d forms a camp diffusion barrier at the apical membrane of the airway epithelium. *The Journal of biological chemistry* 2005;280(9):7997-8003.
36. Lee JH, Richter W, Namkung W, Kim KH, Kim E, Conti M, Lee MG. Dynamic regulation of cystic fibrosis transmembrane conductance regulator by competitive interactions of molecular adaptors. *The Journal of biological chemistry* 2007;282(14):10414-10422.
37. O'Grady SM, Jiang X, Maniak PJ, Birmachu W, Scribner LR, Bulbulian B, Gullikson GW. Cyclic amp-dependent cl secretion is regulated by multiple phosphodiesterase subtypes in human colonic epithelial cells. *The Journal of membrane biology* 2002;185(2):137-144.
38. Liu S, Veilleux A, Zhang L, Young A, Kwok E, Laliberte F, Chung C, Tota MR, Dube D, Friesen RW, et al. Dynamic activation of cystic fibrosis

transmembrane conductance regulator by type 3 and type 4d phosphodiesterase inhibitors. *The Journal of pharmacology and experimental therapeutics* 2005;314(2):846-854.

39. Page CP, Spina D. Selective pde inhibitors as novel treatments for respiratory diseases. *Current opinion in pharmacology* 2012;12(3):275-286.
40. Dunkern TR, Feurstein D, Rossi GA, Sabatini F, Hatzelmann A. Inhibition of tgf-beta induced lung fibroblast to myofibroblast conversion by phosphodiesterase inhibiting drugs and activators of soluble guanylyl cyclase. *European journal of pharmacology* 2007;572(1):12-22.
41. Knudson AG, Jr., Wayne L, Hallett WY. On the selective advantage of cystic fibrosis heterozygotes. *American journal of human genetics* 1967;19(3 Pt 2):388-392.
42. Lipworth BJ. Phosphodiesterase-4 inhibitors for asthma and chronic obstructive pulmonary disease. *Lancet* 2005;365(9454):167-175.
43. Zhang W, Fujii N, Naren AP. Recent advances and new perspectives in targeting cftr for therapy of cystic fibrosis and enterotoxin-induced secretory diarrheas. *Future Med Chem* 2012;4(3):329-345.
44. Dransfield MT, Wilhelm AM, Flanagan B, Tidwell SL, Raju SV, Gaggar A, Steele C, Tang LP, Liu B, Rowe SM. Acquired cftr dysfunction in the lower airways in copd. *Thorax* 2012; Under review.
45. Eckford PD, Li C, Ramjeesingh M, Bear CE. Cystic fibrosis transmembrane conductance regulator (cftr) potentiator vx-770 (ivacaftor) opens the defective channel gate of mutant cftr in a phosphorylation-dependent but atp-independent manner. *The Journal of biological chemistry* 2012;287(44):36639-36649.
46. Jih KY, Hwang TC. Vx-770 potentiates cftr function by promoting decoupling between the gating cycle and atp hydrolysis cycle. *Proceedings of the National Academy of Sciences of the United States of America* 2013;110(11):4404-4409.
47. Le Gars M, Descamps D, Roussel D, Saussereau E, Guillot L, Ruffin M, Tabary O, Hong SS, Boulanger P, Paulais M, et al. Neutrophil elastase degrades cystic fibrosis transmembrane conductance regulator via calpains and disables channel function in vitro and in vivo. *Am J Respir Crit Care Med* 2012.
48. Bodas M, Min T, Mazur S, Vij N. Critical modifier role of membrane-cystic fibrosis transmembrane conductance regulator-dependent ceramide signaling in lung injury and emphysema. *J Immunol* 2011;186(1):602-613.
49. Bradbury NA, Jilling T, Berta G, Sorscher EJ, Bridges RJ, Kirk KL. Regulation of plasma membrane recycling by cftr. *Science* 1992;256(5056):530-532.
50. Mata M, Sarria B, Buenestado A, Cortijo J, Cerda M, Morcillo EJ. Phosphodiesterase 4 inhibition decreases muc5ac expression induced by epidermal growth factor in human airway epithelial cells. *Thorax* 2005;60(2):144-152.
51. Di Benedetto G, Manara-Shediak FS, Mehta A. Effect of cyclic amp on ciliary activity of human respiratory epithelium. *The European respiratory journal* :

*official journal of the European Society for Clinical Respiratory Physiology*  
1991;4(7):789-795.

52. Kwak HJ, Song JS, Heo JY, Yang SD, Nam JY, Cheon HG. Roflumilast inhibits lipopolysaccharide-induced inflammatory mediators via suppression of nuclear factor-kappaB, p38 mitogen-activated protein kinase, and c-jun N-terminal kinase activation. *The Journal of pharmacology and experimental therapeutics* 2005;315(3):1188-1195.

53. Hatzelmann A, Schudt C. Anti-inflammatory and immunomodulatory potential of the novel pde4 inhibitor roflumilast in vitro. *The Journal of pharmacology and experimental therapeutics* 2001;297(1):267-279.

**Figure Legends:**

**Figure 1. Dose-dependent effects of whole cigarette smoke on ion transport function.** Well-differentiated non-CF primary human bronchial epithelial cells were exposed to varying exposures of WCS or air control and then studied in Ussing chambers under short-circuit current (Isc) conditions. **(A)** Representative Isc tracing of HBE cells exposed to WCS for 0, 10, 20, or 30 min. Experiment included serial addition of amiloride (100  $\mu$ M), chloride secretory gradient with amiloride, the cAMP agonist forskolin (20  $\mu$ M), followed by CFTR<sub>Inh</sub>-172 (10  $\mu$ M) to confirm CFTR dependence. **(B)** Forskolin stimulated change in Isc is shown for each shown cigarette smoke exposure level. \*P<0.05, \*\*P<0.005, N=4 per concentration. **(C)** Transepithelial resistance of HBE monolayers at the start of the experiment. \*\*P<0.005, \*P<0.05, N=4.

**Figure 2. Activation of CFTR by roflumilast.** **(A)** Representative Isc tracing of well differentiated non-CF primary human bronchial epithelial cells studied in Ussing chambers under short-circuit current (Isc) conditions. Experiment included serial addition of amiloride (100  $\mu$ M), chloride secretory gradient with amiloride, increasing concentrations of roflumilast or vehicle control, followed by CFTR<sub>Inh</sub>-172 (10  $\mu$ M). **(B)** Summary data of that shown in A. The EC<sub>50</sub> was 2.9 nM. N=4. **(C)** Representative Isc tracing of a normal human bronchus analyzed for CFTR-dependent ion transport under short-circuit current (Isc) conditions. Experiment included serial addition of amiloride (100  $\mu$ M), roflumilast (30 nM) or vehicle control followed by CFTR<sub>Inh</sub>-172 (10  $\mu$ M). **(D)** Summary data of that

shown in C. \* $P < 0.05$ ,  $N = 4$ . **(E)** Representative Isc tracing of differentiated Calu-3 cells studied in Ussing chambers under short-circuit (Isc) conditions. Experiment included serial addition of amiloride (100  $\mu\text{M}$ ), chloride secretory gradient with amiloride, roflumilast (30 nM) or vehicle control, followed by increasing concentrations of forskolin (1 nM – 10  $\mu\text{M}$ ), and CFTR<sub>inh</sub>-172 (10  $\mu\text{M}$ ). **(F)** Summary data of that shown in E, depicting change in Isc in response to increasing forskolin exposure. \* $P < 0.05$ , \*\*\* $P < 0.0005$ .

**Figure 3. Roflumilast increases intracellular cAMP, resulting in CFTR regulatory region phosphorylation.** **(A)** Differentiated Calu-3 cells were exposed to roflumilast (30 nM) or vehicle control, then intracellular cAMP estimated compared to a relative standard curve.  $N = 6$ , \* $P < 0.05$ . **(B)** COS7 cells transfected with a plasmid encoding for the CFTR R-region with an N-terminal HA epitope were treated with increasing concentrations of roflumilast or the PKA antagonist H89 (10  $\mu\text{M}$ ). Immunoblot shown with closed arrow denoting phosphorylated R-region, and open arrow denoting unphosphorylated R-region. N.T.=no treatment. One of three experimental replicates.

**Figure 4. Roflumilast increases short-circuit current in primary human bronchial epithelial monolayers exposed to whole cigarette smoke.** **(A-B)** Non-CF HBE monolayers were exposed to WCS, then studied under short circuit conditions in the setting of amiloride (100  $\mu\text{M}$ ) and a chloride secretory gradient. The change in anion transport was measured following addition of roflumilast (30

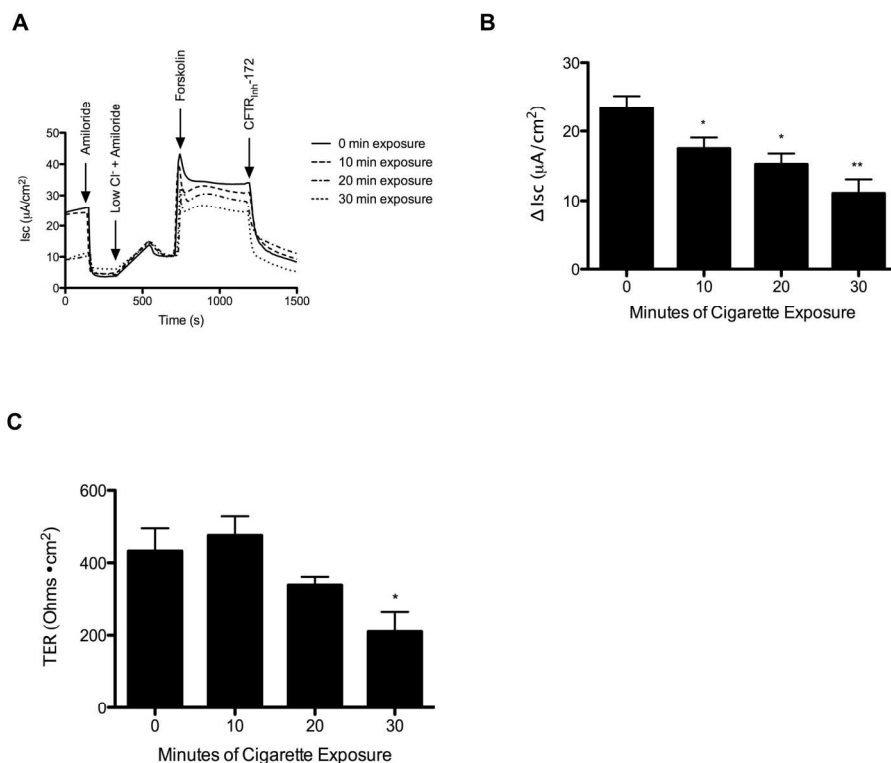
nM) or vehicle control, and plotted as a fraction of forskolin (20  $\mu$ M) mediated activation in air-exposed cells. Agonist-mediated change in I<sub>sc</sub> is plotted for cells exposed to 10 minute (A) and 20 minute (B) WCS exposure times. \*P<0.05, \*\*P<0.005, n=8 per condition. **(C)** Change in forskolin-dependent I<sub>sc</sub> in HBE exposed to 10 min of WCS, and activated with roflumilast (30 nM), ivacaftor (10  $\mu$ M), or a combination of the two under conditions shown in A. \*P<0.05, \*\*P<0.005, \*\*\*P<0.001, n=4 per condition.

**Figure 5. Effect of roflumilast and whole cigarette smoke exposure on airway surface liquid depth.****(A)** Representative confocal Z-scan image of well-differentiated non-CF HBE cells exposed to air control or WCS (10 minutes) and treated with roflumilast (30 nM) or vehicle to the basolateral compartment for 24 hours prior to assay. **(B)** Summary data of ASL depth across experiments shown. \*P<0.05, n=6 monolayers per condition.

**Figure 6. The effect of roflumilast on CFTR-mediated intestinal fluid secretion.****(A)** Representative I<sub>sc</sub> tracing of differentiated T84 intestinal epithelial cells studied in Ussing chambers under short-circuit current (I<sub>sc</sub>) conditions. Experiment included serial addition of amiloride (100  $\mu$ M), chloride secretory gradient with amiloride, roflumilast (30 nM) or vehicle control followed by CFTR<sub>Inh</sub>-172 (10  $\mu$ M). **(B)** Summary data of change in stimulated I<sub>sc</sub> as shown in A. \*P<0.05, N=6 per condition. **(C)** Representative photograph of ligated CFTR +/- mouse intestine following 3 hour incubation with roflumilast (30 nM) or

vehicle control in DMEM vigorously gassed with 95% O<sub>2</sub>/5% CO<sub>2</sub> and held at 37 °C. Scale bar is 1 cm. **(D)** Summary data of relative wet/dry ratio of murine intestine CFTR +/+ and CFTR -/- mice following 3 hr incubation with test compounds. Forskolin control was 20 μM exposure. **(E)** Change in diameter of ligated intestine following 3 hour incubation as detected by investigator blinded to treatment assignment. \*P<0.05, \*\*P<0.005, n=6 per condition.

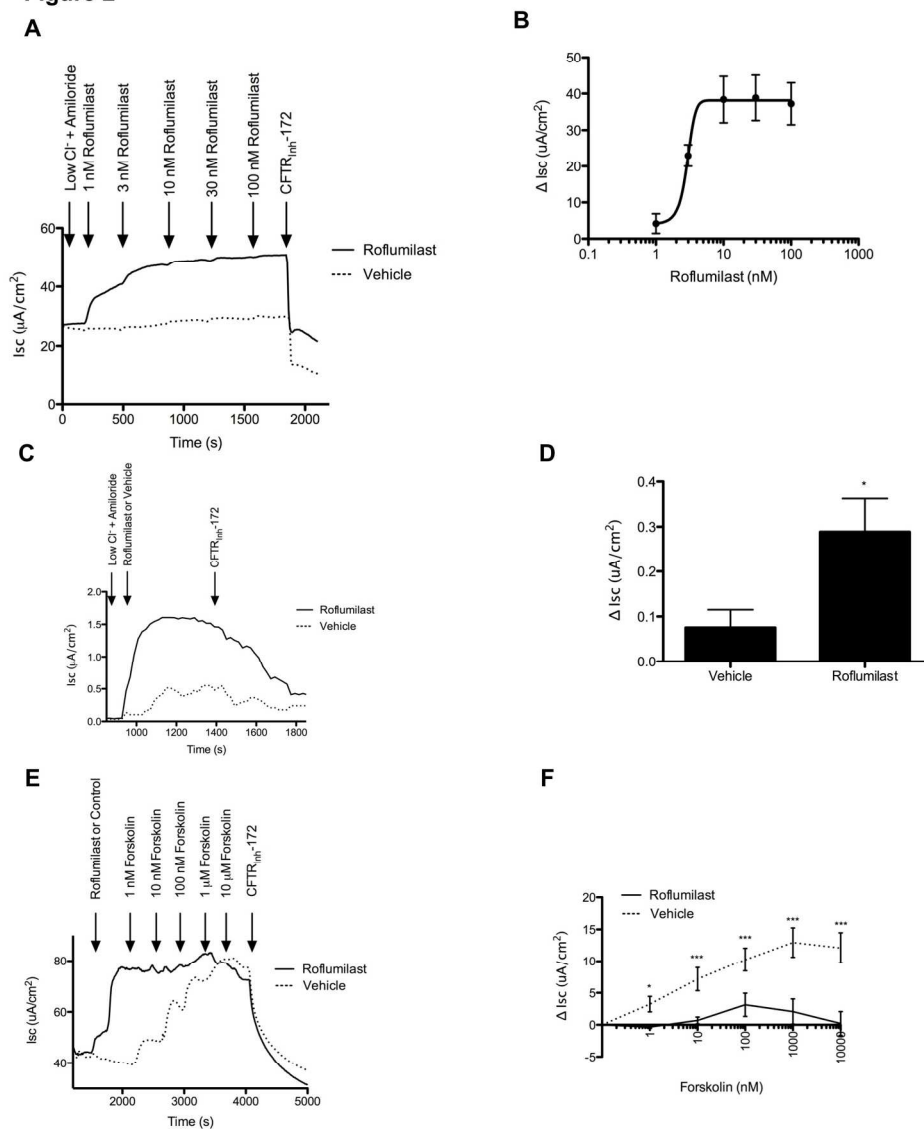
Figure 1



Dose-dependent effects of whole cigarette smoke on ion transport function. Well-differentiated non-CF primary human bronchial epithelial cells were exposed to varying exposures of WCS or air control and then studied in Ussing chambers under short-circuit current (Isc) conditions. (A) Representative Isc tracing of HBE cells exposed to WCS for 0, 10, 20, or 30 min. Experiment included serial addition of amiloride (100  $\mu\text{M}$ ), chloride secretory gradient with amiloride, the cAMP agonist forskolin (20  $\mu\text{M}$ ), followed by CFTR<sub>inh</sub>-172 (10  $\mu\text{M}$ ) to confirm CFTR dependence. (B) Forskolin stimulated change in Isc is shown for each shown cigarette smoke exposure level. \* $P < 0.05$ , \*\* $P < 0.005$ ,  $N = 4$  per concentration. (C) Transepithelial resistance of HBE monolayers at the start of the experiment. \*\* $P < 0.005$ , \* $P < 0.05$ ,  $N = 4$ .

184x165mm (300 x 300 DPI)

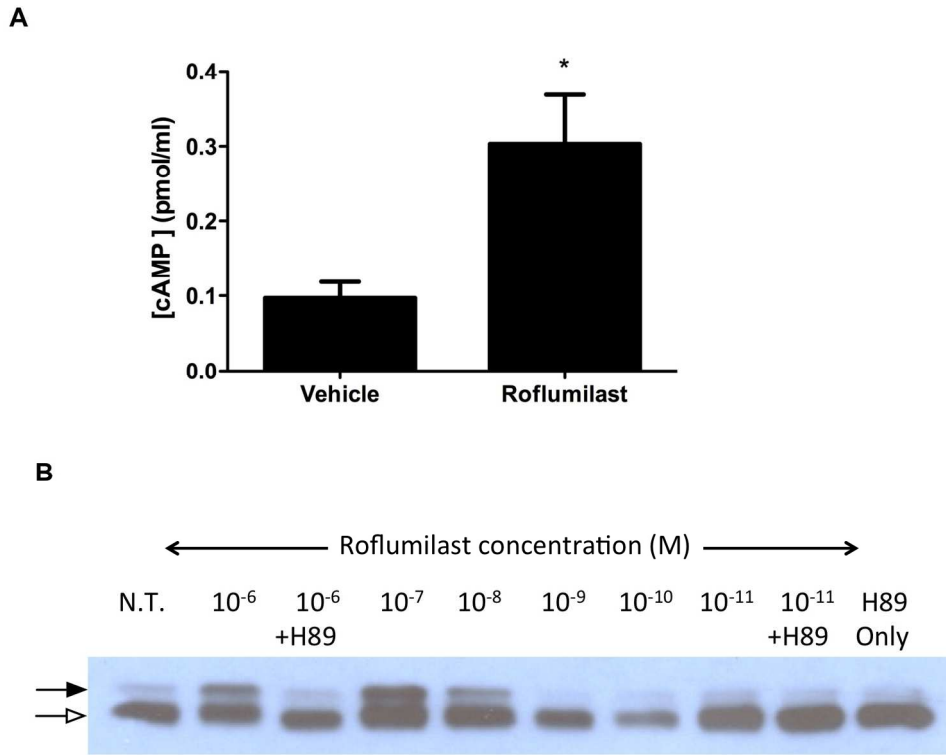
Figure 2



Activation of CFTR by roflumilast. (A) Representative Isc tracing of well differentiated non-CF primary human bronchial epithelial cells studied in Ussing chambers under short-circuit current (Isc) conditions. Experiment included serial addition of amiloride (100 μM), chloride secretory gradient with amiloride, increasing concentrations of roflumilast or vehicle control, followed by CFTRInh-172 (10 μM). (B) Summary data of that shown in A. The EC<sub>50</sub> was 2.9 nM. N=4. (C) Representative Isc tracing of a normal human bronchus analyzed for CFTR-dependent ion transport under short-circuit current (Isc) conditions. Experiment included serial addition of amiloride (100 μM), roflumilast (30 nM) or vehicle control followed by CFTRInh-172 (10 μM). (D) Summary data of that shown in C. \*P<0.05, N=4. (E) Representative Isc tracing of differentiated Calu-3 cells studied in Ussing chambers under short-circuit (Isc) conditions. Experiment included serial addition of amiloride (100 μM), chloride secretory gradient with amiloride, roflumilast (30 nM) or vehicle control, followed by increasing concentrations of forskolin (1 nM – 10 μM), and CFTRInh-172 (10 μM). (F) Summary data of that shown in E, depicting change in Isc in response to increasing forskolin exposure. \*P<0.05, \*\*\*P<0.0005.

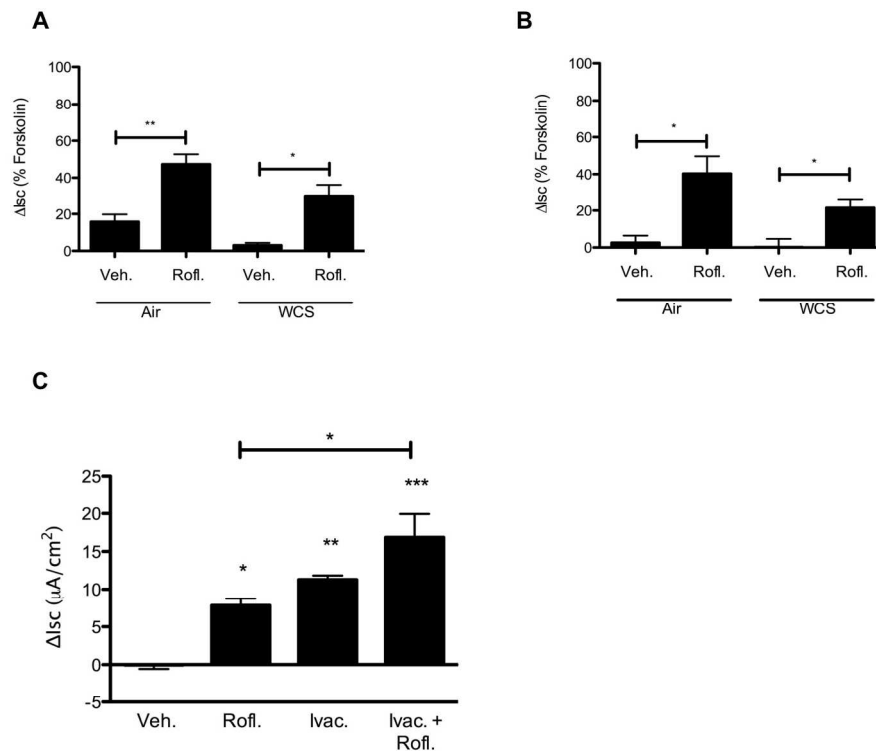
177x215mm (300 x 300 DPI)

Figure 3



Roflumilast increases intracellular cAMP, resulting in CFTR regulatory region phosphorylation. (A) Differentiated Calu-3 cells were exposed to roflumilast (30 nM) or vehicle control, then intracellular cAMP estimated compared to a relative standard curve. N=6, \*P<0.05. (B) COS7 cells transfected with a plasmid encoding for the CFTR R-region with an N-terminal HA epitope were treated with increasing concentrations of roflumilast or the PKA antagonist H9 (10  $\mu$ M). Immunoblot shown with closed arrow denoting phosphorylated R-region, and open arrow denoting unphosphorylated R-region. N.T.=no treatment. One of three experimental replicates. 162x146mm (300 x 300 DPI)

Figure 4

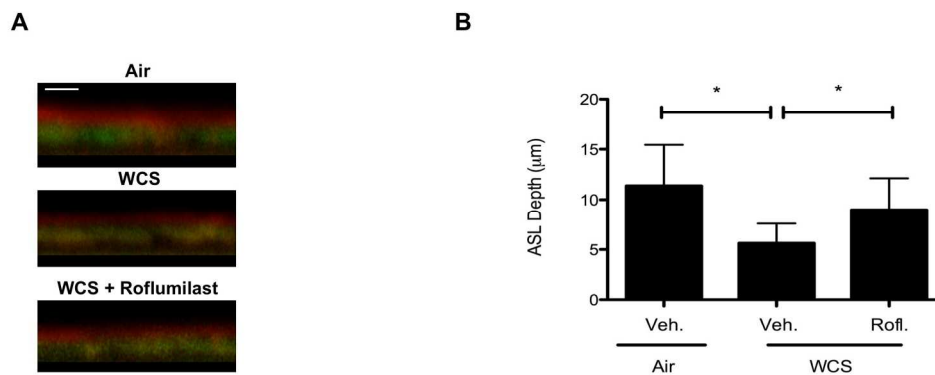


Roflumilast increases short-circuit current in primary human bronchial epithelial monolayers exposed to whole cigarette smoke. (A-B) Non-CF HBE monolayers were exposed to WCS, then studied under short circuit conditions in the setting of amiloride (100  $\mu M$ ) and a chloride secretory gradient. The change in anion transport was measured following addition of roflumilast (30 nM) or vehicle control, and plotted as a fraction of forskolin (20  $\mu M$ ) mediated activation in air-exposed cells. Agonist-mediated change in  $I_{sc}$  is plotted for cells exposed to 10 minute (A) and 20 minute (B) WCS exposure times. \* $P < 0.05$ , \*\* $P < 0.005$ ,  $n = 8$  per condition. (C) Change in forskolin-dependent  $I_{sc}$  in HBE exposed to 10 min of WCS, and activated with roflumilast (30 nM), ivacaftor (10  $\mu M$ ), or a combination of the two under conditions shown in A.

\* $P < 0.05$ , \*\* $P < 0.005$ , \*\*\* $P < 0.001$ ,  $n = 4$  per condition.

181x160mm (300 x 300 DPI)

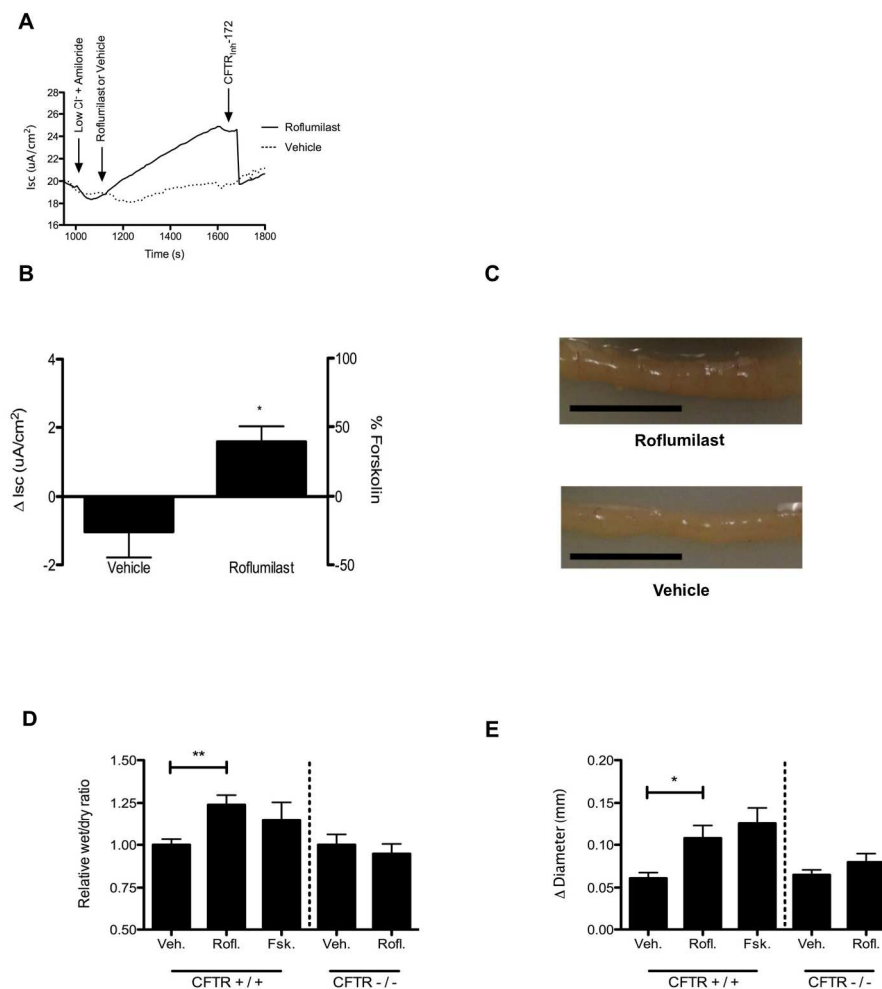
Figure 5



Effect of roflumilast and whole cigarette smoke exposure on airway surface liquid depth. (A) Representative confocal Z-scan image of well-differentiated non-CF HBE cells exposed to air control or WCS (10 minutes) and treated with roflumilast (30 nM) or vehicle to the basolateral compartment for 24 hours prior to assay. (B) Summary data of ASL depth across experiments shown. \* $P < 0.05$ ,  $n = 6$  monolayers per condition.

176x88mm (300 x 300 DPI)

Figure 6



The effect of roflumilast on CFTR-mediated intestinal fluid secretion. (A) Representative Isc tracing of differentiated T84 intestinal epithelial cells studied in Ussing chambers under short-circuit current (Isc) conditions. Experiment included serial addition of amiloride (100  $\mu$ M), chloride secretory gradient with amiloride, roflumilast (30 nM) or vehicle control followed by CFTR<sub>inh</sub>-172 (10  $\mu$ M). (B) Summary data of change in stimulated Isc as shown in A. \* $P < 0.05$ ,  $N = 6$  per condition. (C) Representative photograph of ligated CFTR +/+ mouse intestine following 3 hour incubation with roflumilast (30 nM) or vehicle control in DMEM vigorously gassed with 95% O<sub>2</sub>/5% CO<sub>2</sub> and held at 37 °C. Scale bar is 1 cm. (D) Summary data of relative wet/dry ratio of murine intestine CFTR +/+ and CFTR -/- mice following 3 hr incubation with test compounds. Forskolin control was 20  $\mu$ M exposure. (E) Change in diameter of ligated intestine following 3 hour incubation as detected by investigator blinded to treatment assignment. \* $P < 0.05$ , \*\* $P < 0.005$ ,  $n = 6$  per condition.

192x215mm (300 x 300 DPI)

## Online Data Supplement

### CFTR Activation By Roflumilast Contributes to Therapeutic Benefit in Chronic Bronchitis

James A Lambert, S Vamsee Raju, Li Ping Tang, Carmel M McNicholas, Yao Li, Clifford W Courville, George E Coricor, Roopan F Faris, Lisa H Smoot, Marina M Mazur, Graeme B Bolger, Steven M Rowe

#### Methods

##### *Characterization of whole cigarette smoke exposure*

Exposure to mainstream cigarette smoke aerosol concentration was determined by filtration. The Scireq inhalation exposure plenum directly provided sequential filter samples. Briefly, aluminum filter holders (In-Tox Products, LLC,

Albuquerque, NM) held Pallflex® T60A20 47 mm filters and used an isoaxial exhaust port located on the plenum to collect sample. Collection of sample times ranged from three to ten minutes. Volumetric flow rate of the filter sample was determined prior to each test using a Defender 520 primary flow calibration device (BIOS International, Butler, NJ). A Model MX5 analytical microbalance (Mettler Toledo, Columbus, OH) determined the filter tare prior to sample collection using and final weights. The following equation was utilized to determine the mass per unit volume cigarette smoke aerosol concentration (C):

$$C = \frac{\text{filter net weight (mg)}}{\text{filter sample volume (L)}} \times 1000 \frac{\mu\text{g}}{\text{mg}}$$

Filter net weight = filter final weight – filter tare weight

Filter sample volume = filter sampler volumetric flow rate (L/min) × filter sample collection duration (min)

The mean cigarette smoke aerosol concentration during exposures in which one cigarette was smoked every 10 min and the particulate matter was found to be  $74.16 \pm 7.12 \mu\text{g/L}$ . Aerosol concentration was determined during exposure by collecting condensates on filters connected to the exhaust of the exposure chamber using an isoaxial sample collection port. The inExpose system was assembled inside a Class II Type A2 biosafety cabinet. All flow rates were calibrated using the Defender primary flow calibration device and recorded. Relative aerosol particle concentration was monitored using the MicroDust Pro Aerosol Monitor (Casella, England). Actual concentration was determined using 47 mm Filter Samplers (In-Tox Products, Moriarty, NM) that contained PallFlex Membrane Filters (Pall, T60A20) and found to be a lower concentration relative to other cigarette smoke-centered studies. Additionally, the particle size was determined using a seven stage In-Tox Impactor (In-Tox Products, Moriarty, NM). The relative particle concentrations versus time plots for each microdust sample are shown in Supplement Figure 1

*CFTR Measurements in primary human bronchial epithelial cells*

IRB approved human cell culture use. Lung explant derived primary HBE cells were obtained after written informed consent from CF and non-CF subjects by methods described previously (1). Cell monolayers were grown at an air-liquid interface until terminally differentiated. Using MC8 clamps and P2300 Ussing chambers (Physiologic Instruments, San Diego, CA) (2),  $I_{sc}$  was measured under voltage clamp conditions. CFTR activity was measured by the change in  $I_{sc}$  upon stimulation with roflumilast (30nM) or vehicle in the setting of amiloride (100  $\mu$ M) and a  $Cl^-$  secretory gradient, where indicated; CFTR<sub>Inh</sub>-172 was used to confirm CFTR dependence.

## Legends

**Supplement Figure 1. Whole Cigarette Exposure Characterization.** Temporal pattern of cigarette smoke generated by automated smoking machine was analyzed by MicroDust Pro Aerosol Monitor (Casella, England) and the time versus relative particulate matter is plotted for 3 different replicates.

**Supplement Figure 2. Effects of roflumilast on CFTR expression.**

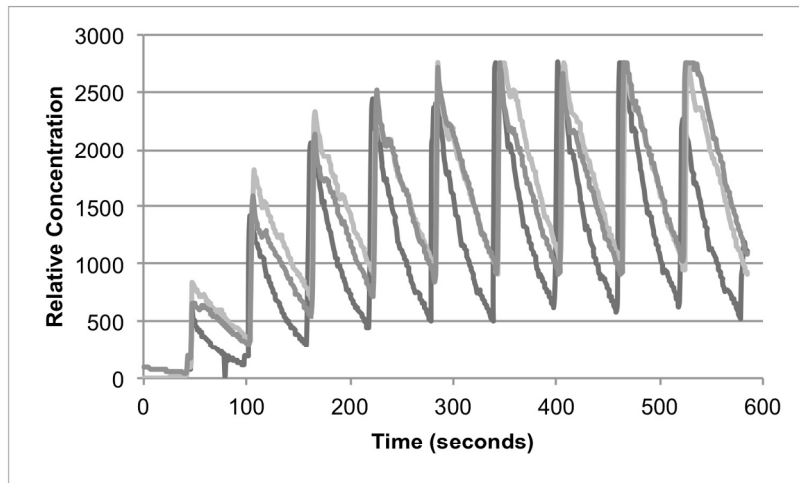
Western blot analysis of cell lysates of primary human bronchial epithelial cells treated with DMSO vehicle control or roflumilast for 24 hours. CFTR bands B and C are shown by the black and white arrows, respectively. Densitometric analysis indicated no difference in CFTR protein expression. P=NS.

**Supplement Figure 3. Effect of roflumilast on CFTR open channel probability.**

(A) Inside-out membrane patches were obtained from primary human bronchial epithelial cells expressing wild-type CFTR. Single channel conductance tracings recorded with 75 nM PKA +1 mM ATP alone or 75 nM PKA +1 mM ATP + 30 nM roflumilast. (B) Summary of open channel probability with and without roflumilast. N=9, P=NS.

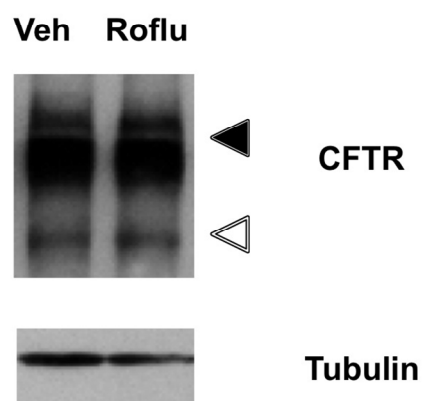
## References

1. Van Goor F, Hadida S, Grootenhuis PD, Burton B, Cao D, Neuberger T, Turnbull A, Singh A, Joubran J, Hazlewood A, et al. Rescue of cf airway epithelial cell function in vitro by a cftr potentiator, vx-770. *Proceedings of the National Academy of Sciences of the United States of America* 2009;106(44):18825-18830.
2. Rowe SM, Pyle LC, Jurkevante A, Varga K, Collawn J, Sloane PA, Woodworth B, Mazur M, Fulton J, Fan L, et al. Deltaf508 cftr processing correction and activity in polarized airway and non-airway cell monolayers. *Pulm Pharmacol Ther.*

**Supplement Figure 1**

Whole Cigarette Exposure Characterization. Temporal pattern of cigarette smoke generated by automated smoking machine was analyzed by MicroDust Pro Aerosol Monitor (Casella, England) and the time versus relative particulate matter is plotted for 3 different replicates.  
158x107mm (300 x 300 DPI)

## Supplementary Figure 2

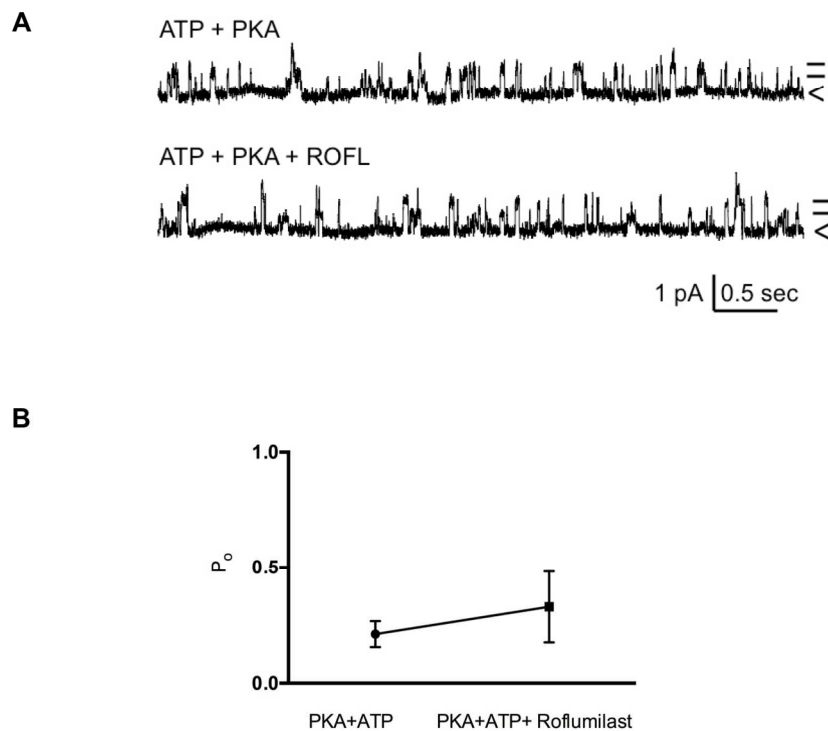


Effects of roflumilast on CFTR expression.

Western blot analysis of cell lysates of primary human bronchial epithelial cells treated with DMSO vehicle control or roflumilast for 24 hours. CFTR bands B and C are shown by the black and white arrows, respectively. Densitometric analysis indicated no difference in CFTR protein expression. P=NS.

119x73mm (300 x 300 DPI)

## Supplementary Figure 3



Effect of roflumilast on CFTR open channel probability.

(A) Inside-out membrane patches were obtained from primary human bronchial epithelial cells expressing wild-type CFTR. Single channel conductance tracings recorded with 75 nM PKA +1 mM ATP alone or 75 nM PKA +1 mM ATP + 30 nM roflumilast. (B) Summary of open channel probability with and without roflumilast. N=9, P=NS.

158x137mm (300 x 300 DPI)